



# Rapporti tecnici INGV

Time occurrence of  
earthquake instabilities in  
rate- and state-dependent friction models

# 192



Istituto Nazionale di  
Geofisica e Vulcanologia

## **Direttore**

Enzo Boschi

## **Editorial Board**

Raffaele Azzaro (CT)

Sara Barsotti (PI)

Mario Castellano (NA)

Viviana Castelli (BO)

Rosa Anna Corsaro (CT)

Luigi Cucci (RM1)

Mauro Di Vito (NA)

Marcello Liotta (PA)

Simona Masina (BO)

Mario Mattia (CT)

Nicola Pagliuca (RM1)

Umberto Sciacca (RM1)

Salvatore Stramondo (CNT)

Andrea Tertulliani - Editor in Chief (RM1)

Aldo Winkler (RM2)

Gaetano Zonno (MI)

## **Segreteria di Redazione**

Francesca Di Stefano - coordinatore

Tel. +39 06 51860068

Fax +39 06 36915617

Rossella Celi

Tel. +39 06 51860055

Fax +39 06 36915617

[redazionecen@ingv.it](mailto:redazionecen@ingv.it)



# Rapporti tecnici INGV

## TIME OCCURRENCE OF EARTHQUAKE INSTABILITIES IN RATE- AND STATE-DEPENDENT FRICTION MODELS

Andrea Bizzarri<sup>1</sup>, Paola Crupi<sup>2</sup>, Salvatore de Lorenzo<sup>2</sup>, Mariano Loddo<sup>2</sup>

<sup>1</sup>INGV (Istituto Nazionale di Geofisica e Vulcanologia, Sezione di Bologna)

<sup>2</sup>UNIVERSITÀ DEGLI STUDI DI BARI (Dipartimento di Geologia e Geofisica)

# 192



## Table of contents

Introduction	5
1. The spring–slider dashpot model of a seismogenic fault	6
2. Rate– and state–dependent friction laws	6
2.1. Dietrich–Ruina’s model	7
2.2. Ruina’s model	7
2.3. Chester–Higgs’ model	7
2.4. Frozen friction above $v_c$	8
3. Numerical results	8
4. Summary	13
References	15



## Introduction

Since the latter half of last century many studies and laboratory experiments have focused on the understanding of the evolution of frictional strength during sliding events on active faults. Such events may occur through aseismic fault creep, high-velocity slip and, in some cases, as a combination of both.

According to the concept that earthquakes are frictional instabilities, their time occurrence may show a periodical pattern (the seismic cycle) whose behavior can be referred to the stick-slip dynamic. The dynamic evolution of a fault is often modeled considering its formal analogy with a physical system known as the spring-slider model (namely, a damped harmonic oscillator). Many experimental studies have been conducted using the spring-slider model, most of them simulating the interaction between slip surfaces with the surrounding elastic medium with a single-degree-of-freedom system. Despite its obvious limitations, such a model has provided important insights on dynamics of stick-slip cycle [Gu et al., 1984; Carlson et al., 1994], nucleation of earthquakes and triggered earthquake phenomena [e.g. Belardinelli et al., 2003].

On the basis of several experimental results on rock friction, Dieterich [1979] and Ruina [1983] formulated rate- and state-dependent friction laws, in which the frictional resistance is expressed through the evolution of the sliding rate and its history. Afterwards, Chester and Higgs [1992] figured out that also the temperature variation, produced by frictional heating, can affect the duration of the seismic cycle and the evolution of the frictional strength as well and consequently they incorporate such a thermal effect, improving the previous Ruina's constitutive law.

The present study is aimed to:

1. investigate the spring-slider physical response depending on the adopted constitutive law;
2. show the influence that the constitutive laws can exert on the time occurrence of a seismic instability and on the seismic cycle duration;
3. compare the constitutive laws in order to show their different features in simulating the evolution of slip velocity, stress drop and seismic cycle.

## 1. The spring–slider dashpot model of a seismogenic fault

In the present study the equation of motion of a spring-slider dynamic system, including the inertial term, is numerically solved:

$$m\ddot{u} = k(u_{load} - u) - \tau \quad (1)$$

The spring-slider model here considered is the same as that one introduced in many previous works dealing with fault dynamics where the model is deeply discussed; here we will shortly describe it for completeness.

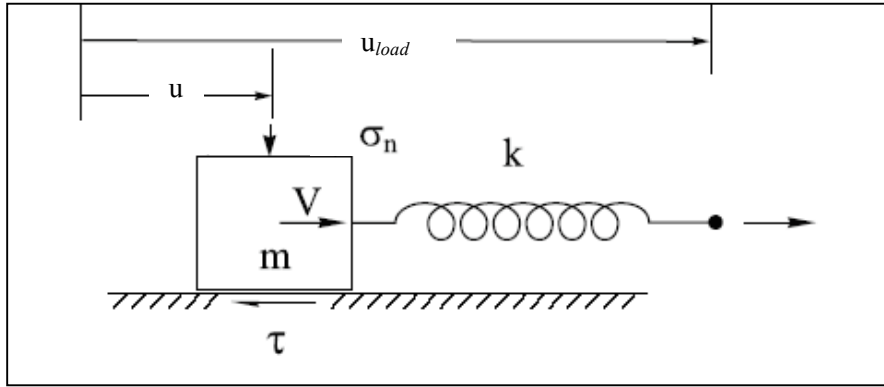


**Figure 1.** Schematic representation of a spring-slider system.

As the name implies, such a model is mainly composed by a rigid block, a spring and a support base (which represents the interface between the bottom of the sliding block and the underlying floor representing a fault plane), and the spring mimicking the elastic medium surrounding the fault. Focusing on Figure 1,  $u$  is the slip,  $m$  is the mass per unit of area,  $\tau$  is the frictional resistance,  $u_{load}$  is the load point displacement and  $k$  is the elastic spring constant.

In order to better understand the evolution of unstable sliding events and their time occurrence, it is necessary to have a description of the motion along the fault, either at low or high speeds. For this purpose according to the simulation strategy employed by Boatwright and Cocco [1996] and by Belardinelli et al., [2003], the equation of motion is solved for the quasi-static regime and also for the dynamic one both separated by the physical quantity called critical velocity  $v_c$ . In particular, as long as the slip rate is lower than the critical velocity ( $v \leq v_c$ ) the dynamic equation is solved in the quasi-static approximation (i.e., by neglecting the inertial term  $m\ddot{u}$  in equation (1)), and when  $v > v_c$  the motion is fully dynamic and the complete equation (1) is solved.

When the slider velocity reaches large values (compared to the loading point velocity), a seismic instability occurs. In particular, a seismic slip event, or an instability, is considered to occur when the slip velocity becomes transiently larger than an assumed threshold velocity, referred to as  $v_L$  [Belardinelli et al., 2003; Bizzarri, 2010c]. In a long time interval the slider can be characterized by a periodical variation of values of frictional resistance and sliding velocity. Such a periodical variation defines the slider cycle time ( $T_{cycle}$ ), calculated as the interval separating two subsequent time instants when the slip rate overcomes  $v_L$ . In the present study the  $T_{cycle}$  represents an important physical quantity because it is closely related to the earthquake recurrence time on the same fault [Belardinelli et al., 2003; Bizzarri, 2010c].

## 2. Rate– and state–dependent friction laws

So far many studies stated that unstable failures and earthquakes are the result of interactions between the frictional properties of a sliding surface with the surrounding elastic system [Weeks, 1993]. Moreover,



laboratory experiments have showed some dependences of the friction on the sliding rate and on the sliding history that are critical to the frictional stability of faults. Furthermore, considerable progresses have been made in the understanding of fault dynamics and rock friction since constitutive equations including such sliding history and velocity have been first introduced [Dieterich, 1979; Ruina, 1983]. These constitutive equations were developed in order to reproduce many frictional behaviors observed in rocks during experiments and afterwards have been used also to simulate and model many aspects of faults seismicity.

In the present study we will consider three different analytical formulations of the rate- and state-dependent friction laws: the Dieterich-Ruina's law (DR henceforth), the Ruina's law (RU henceforth) and the Chester-Higgs' law (CH henceforth). While the first two laws do not directly incorporate the effects of the frictional heat, the Ruina's law has been extended by Chester and Higgs [1992] to account for the temperature variations along the fault.

### 2.1. Dieterich–Ruina's model

One of the most important aspects of such an empirical model was that Dieterich, through his laboratory experiments, figured out a logarithmic dependence of the frictional strength on the sliding velocity [Weeks, 1993]. The DR law, also known as the ageing evolution law, is expressed through the following equation:

$$\left\{ \begin{array}{l} \tau = \left[ \mu_* + a \ln\left(\frac{v}{v_*}\right) + b \ln\left(\frac{\psi v_*}{L}\right) \right] \sigma_n^{eff} \\ \frac{d\psi}{dt} = 1 - \frac{\psi v}{L} \end{array} \right. \quad (2)$$

In the above equation  $\tau$  is the frictional resistance of a sliding surface which depends on the constant frictional coefficient  $\mu_*$  considered at a reference slip rate  $v_*$  and on two governing parameters  $a$  and  $b$ : the former describes the direct dependence of friction on the slip rate and the latter states the evolution effect that the velocity exerts on the frictional strength as well. Moreover,  $\tau$  depends on the characteristic distance  $L$  which controls the evolution of the state variable  $\psi$ , which account for the slip history and for properties of contact sliding surfaces (memory effects). In equation (2)  $v$  is the slip velocity and  $\sigma_n^{eff}$  is the effective normal stress.

### 2.2. Ruina's model

The RU law, also known as the slip evolution law, is expressed as follows:

$$\left\{ \begin{array}{l} \tau = \left[ \mu_* + a \ln\left(\frac{v}{v_*}\right) + \Theta \right] \sigma_n^{eff} \\ \frac{d\Theta}{dt} = -\frac{v}{L} \left[ \Theta + b \ln\left(\frac{v}{v_*}\right) \right] \end{array} \right. \quad (3)$$

The physical meaning of the parameters appearing in equation (3) are the same as those already mentioned for equation (2), except for the state variable  $\Theta$ , which is now a dummy variable and it is not directly associated to the average contact time (hold time) of the micro-asperities of the fault surface.

### 2.3. Chester–Higgs's model

As already mentioned, the effect of the temperature variation on the evolution of frictional strength hasn't been taken into account neither in the DR nor in the RU model. Indeed, Chester and Higgs [1992], interpreted their experiments by suggesting the temperature affects the frictional resistance. Their model reads:

$$\begin{cases} \tau = \left[ \mu_* + a \ln\left(\frac{v}{v_*}\right) + \Theta + \frac{aQ_a}{R} \left( \frac{1}{T^f} - \frac{1}{T_*} \right) \right] \sigma_n^{eff} \\ \frac{d\Theta}{dt} = -\frac{v}{L} \left[ b \ln\left(\frac{v}{v_*}\right) + \Theta + \frac{bQ_b}{R} \left( \frac{1}{T^f} - \frac{1}{T_*} \right) \right] \end{cases} \quad (4)$$

where  $T^f$  is the temperature developed by frictional heat. It is expressed by the closed-form analytical solution of the 1-D Fourier's heat conduction equation, which can be expressed as follows:

$$T \approx T_{ini} + \frac{1}{\rho C \sqrt{\pi \kappa}} \sum_{j=1}^n \tau(t_{j-1}) v(t_{j-1}) \left( \sqrt{t-t_{j-1}} - \sqrt{t-t_j} \right) \quad (5)$$

The equation (5) was originally formulated by Kato [2001], by considering a fault having an infinitesimal thickness and characterized by spatially uniform slip, slip rate and shear stress. In a separate work, Bizzarri [2010b] demonstrated that a more general solution for temperature change, accounting for a fault zone of finite width, reduces to equation (5) in the limit of vanishing slipping zone thickness.

In equation (5)  $T_{ini}$  is the initial uniform temperature (i.e., at  $t = 0$ ),  $\rho$  is the cubic mass density of rocks,  $c$  is the specific heat,  $\kappa$  is the thermal diffusivity of the continuous medium in which the fault is embedded and  $t_0 = 0$  and  $t_n = t$ .

#### 2.4. Frozen friction above $v_c$

In the present study we fully account for low and high velocity values. Originally, Dieterich proposed his constitutive law [Dieterich, 1979, 1981; Weeks, 1993] by considering laboratory experiments performed at relatively low sliding speeds. Weeks [1993] introduced a modification to the steady state analytical expression in the Ruina's rate- and state-dependent friction constitutive law, by postulating that the friction becomes independent of the velocity at high slip rates.

For all the three constitutive laws reported in this study the Weeks' approach has been considered; in this case in equations (2), (3) and (4) we use

$$\ln\left(\frac{v}{v_*}\right) \rightarrow \ln\left(\frac{v_c}{v_*}\right) \text{ when } v \geq v_c \quad (6)$$

Equation (6) states that the velocity  $v$  is frozen at a suitable value of the slider velocity  $v_c$  as soon as such critical threshold is exceeded. For completeness we have also considered the case without any constrains at high slip rates. In the remainder of this study we will refer to the Week's approach as to the frozen (FR) model while the latter will be tagged as the not frozen (NOT FR) model.

### 3. Numerical results

In the present section we present numerical results obtained by solving numerically the equation of motion (1) coupled with the three constitutive laws (DR, RU, CH). As already mentioned previously, the main goals of the present study are:

- a) to analyze the physical meaning of each constitutive law during the different phases of motion along a fault plane, considering the frozen and not frozen approximation;
- b) to check if, and how, each law, with its constrains, can influence the duration of the seismic cycle;
- c) to compare all the simulations results in order to understand their main differences and their prominent features.

Starting from the same initial conditions a twin numerical simulations have been conducted for each constitutive law, in order to obtain the time evolutions of the velocity, shear stress and  $T_{cycle}$ , for both the frozen and not frozen cases.

The initial parameters used in all the numerical simulations are reported in Table 1.

<i>Parameter</i>	<i>Value</i>
<b><i>Model Parameters</i></b>	
Tectonic loading rate, $\dot{\tau}_0 = kv_{load}$	$3.17 \times 10^{-3}$ Pa/s (= 1 bar/yr)
Machine stiffness, $k$	10 MPa/m
Period of the analog freely slipping system, $T_{a.f.} = 2\pi \sqrt{m/k}$	5 s
Critical value of the sliding velocity above which the dynamic regime is considered, $v_c$	0.1 mm/s
Threshold value of the sliding velocity defining the occurrence of an instability, $v_l$	0.1 m/s
<b><i>Fault Constitutive Parameters</i></b>	
Initial effective normal stress, $\sigma_n^{eff}$	30 MPa
Logarithmic direct effect parameter, $a$	0.007
Evolution effect parameter, $b$	0.016
Characteristic scale length, $L$	$1 \times 10^{-2}$ m
Reference value of the friction coefficient, $\mu^*$	0.56
Reference value of the sliding velocity, $v^*$	$3.17 \times 10^{-10}$ m/s
Initial slip velocity, $v_0$	$3.17 \times 10^{-10}$ m/s
Initial shear stress, $\tau_0$	16.8 MPa (= $\mu^* \sigma_n^{eff}$ )
Initial temperature, $T_0$	100 °C
Heat capacity for unit volume of the bulk composite, $c$	$2.6 \times 10^6$ J/(m <sup>3</sup> °C)
Thermal diffusivity, $\kappa$	$1 \times 10^{-6}$ m <sup>2</sup> /s

**Table 1.** Parameters adopted in the present study. Initial values refer to the time  $t = 0$ .

The following figures show the superimposition of the whole ensemble of the numerical experiments carried out for each constitutive equation. We will mainly focus on the time evolution of the slip rate (Figures 2a, 2b), of the shear stress (Figure 3) and of the seismic cycle (Figure 4).

Two important points can be appreciated trough the analysis of Figure 2a:

- the differences between velocity peaks for each constitutive law;
- the different time occurrence of seismic events obtained by assuming the same constitutive law on the fault, but considering frozen or not frozen conditions.

In particular, referring to the velocity peaks, we can see that higher velocities are reached for the instability pertaining to a fault governed by the DR law. Furthermore, the slip velocities obtained for the frozen case are greater than those obtained for the not frozen one, for both DR and CH constitutive laws, while an opposite trend occurs for the RU law.

Besides this result, we want to emphasize that the slip velocities obtained with the CH frozen simulation are in agreement with those obtained for the RU not frozen simulation. Moreover, the CH law requires lower values of both time and slip rate peaks to undergo to a seismic instability, since it considers the thermal effects expressed by equation (5). Finally, we observe that, by considering the same constitutive model, the frozen and not frozen instabilities exhibit quite different patterns that are not in phase with each other over the time.

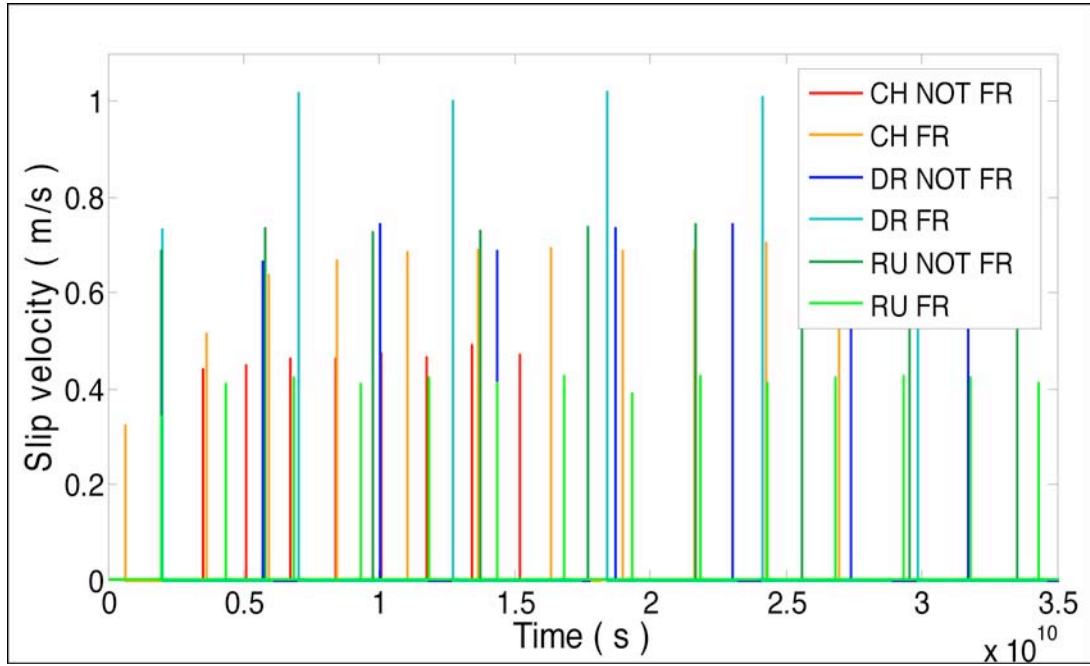


**Figure 2a.** Slip velocity time history in a linear scale. The light and dark red lines represent the CH simulations, the light and dark green lines represent the RU simulations and the light and dark blue lines show the DR simulations.

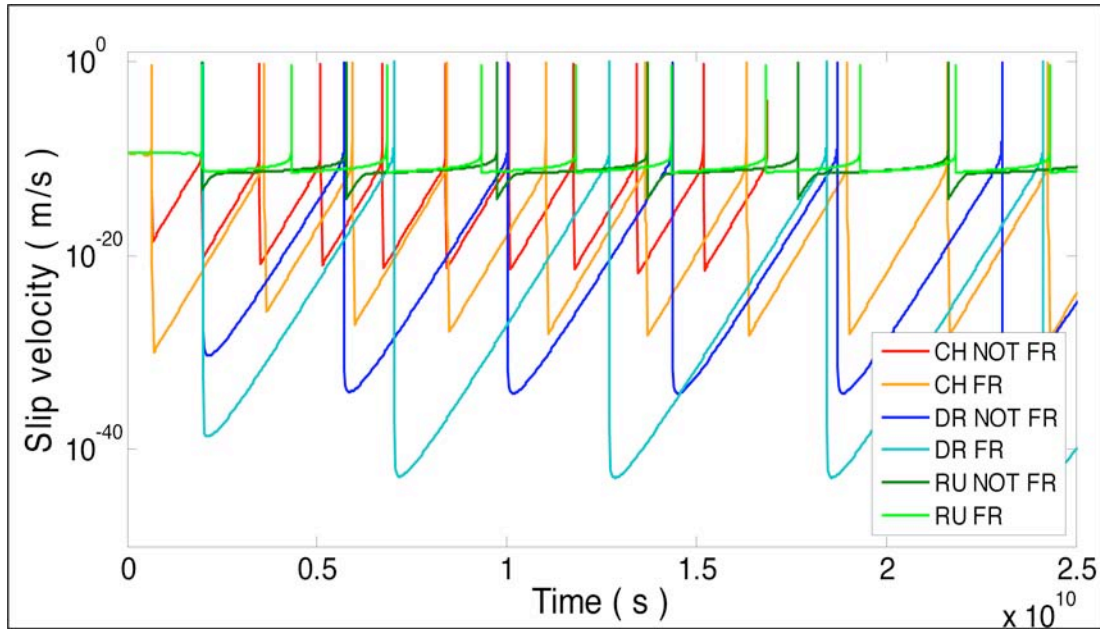


**Figure 2b.** The same as Figure 2a, but now  $v$  is in a logarithmic scale.

Referring to Figure 2b, the semi-logarithmic scale allows to appreciate the differences between the velocity minima reached after each instability. Indeed, according to the previous observations, the lowest minima are those governed by the DR law and, what is more, for both the CH and DR laws the frozen simulations show lower minima with respect to the not frozen case. On the contrary, the opposite happens with the RU simulations. Moreover, by considering the same constitutive law, it can be still appreciated the time lag between the frozen and not frozen slip events.

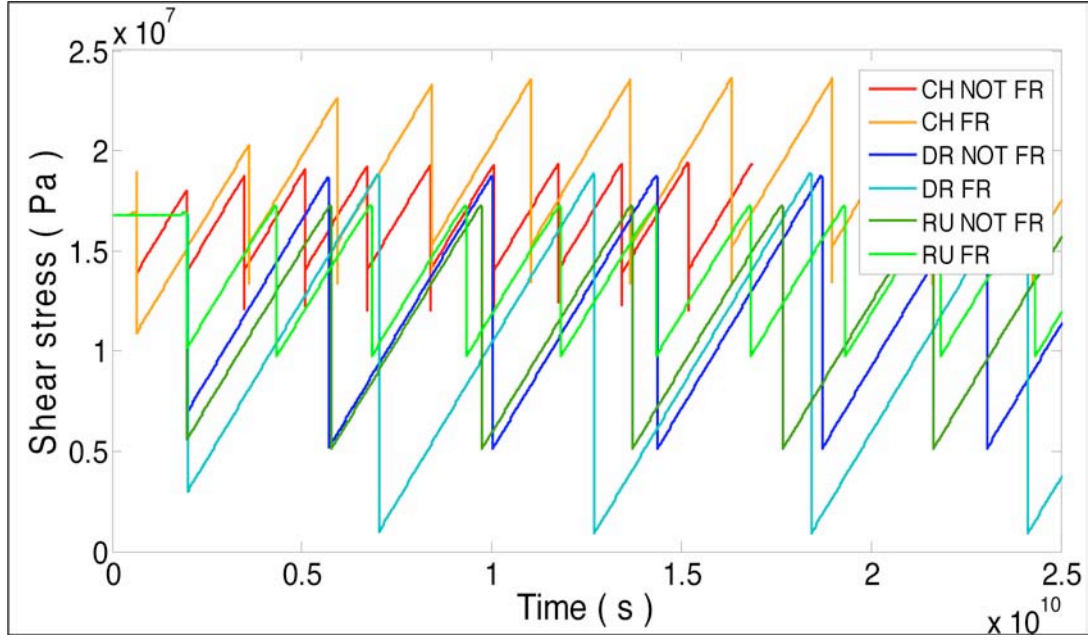


**Figure 3.** Shear stress time history. The colors have the same meaning as in Figures 2a and 2b.

We plot in Figure 3 the time evolution of the resulting traction predicted by the different constitutive models. It can be clearly observed that higher shear stress peaks are obtained with the CH frozen simulation (light red line), while lower shear stress peaks are reached in the RU simulations (light and dark green lines). Moreover, the shear stress peaks reached in both DR and RU simulations are comparable, while the CH frozen peaks are significantly greater than those referred to the CH not frozen simulation. Furthermore, by considering both the DR simulations (frozen and not frozen; light and dark blue lines), the shear stress minima are significantly lower in the frozen constrain. The opposite occurs in the RU simulations, that is the minima turn to be lower in the not frozen case.

Conversely to the previous situations, the traction minima seem to be comparable in both the CH simulations. Interestingly, the stress drop that pertaining to each constitutive law is proportional to the slip velocity peaks (showed in Figure 2a); highest stress drops are associated to the highest slip velocities, realized in the DR simulations.

Referring to the objective b) of the present section, Figure 4 shows the recurrence time of the seismic instabilities for all the constitutive laws, either in frozen and not frozen cases. Here it can be observed that, on average, for both the frozen and not frozen simulations the CH law shows a lower seismic cycle pattern, the DR shows the highest values of seismic cycle while the RU seismic cycle is about in the middle.

Furthermore, while for both CH and DR laws the seismic cycle is smaller in the not frozen case, for the RU law the lower seismic cycle is related in the frozen simulation. Therefore the RU seismic cycle has an opposite trend, compared to the other two constitutive laws, as it can be also seen from Table 2.

Eventually the values of  $T_{cycle}$  predicted by both the RU and CH frozen simulations are nearly comparable. Table 2 summarizes all the seismic cycle values extrapolated for each constitutive law, in order to highlight the opposite trend governing the RU simulation.

<i>Constitutive law</i>	$T_{cycle}$ (yr)	$(T_{cycle}^{(FR)} - T_{cycle}^{(NOT FR)})/T_{cycle}^{(FR)}$ (%)
Dietrich–Ruina frozen	180.9	0,24
Dietrich–Ruina not frozen	137.5	
Ruina frozen	79.2	-0,58
Ruina not frozen	125.6	
Chester–Higgs frozen	84.1	0,36
Chester–Higgs not frozen	54.0	

**Table 2.** Average values of the seismic cycle for each constitutive law and for both the frozen and not frozen cases.  $T_{cycle}$  is computed in all cases starting from the 5<sup>th</sup> instability event, in order to avoid possible effects of the transient stage of the system, basically controlled by the initial conditions.

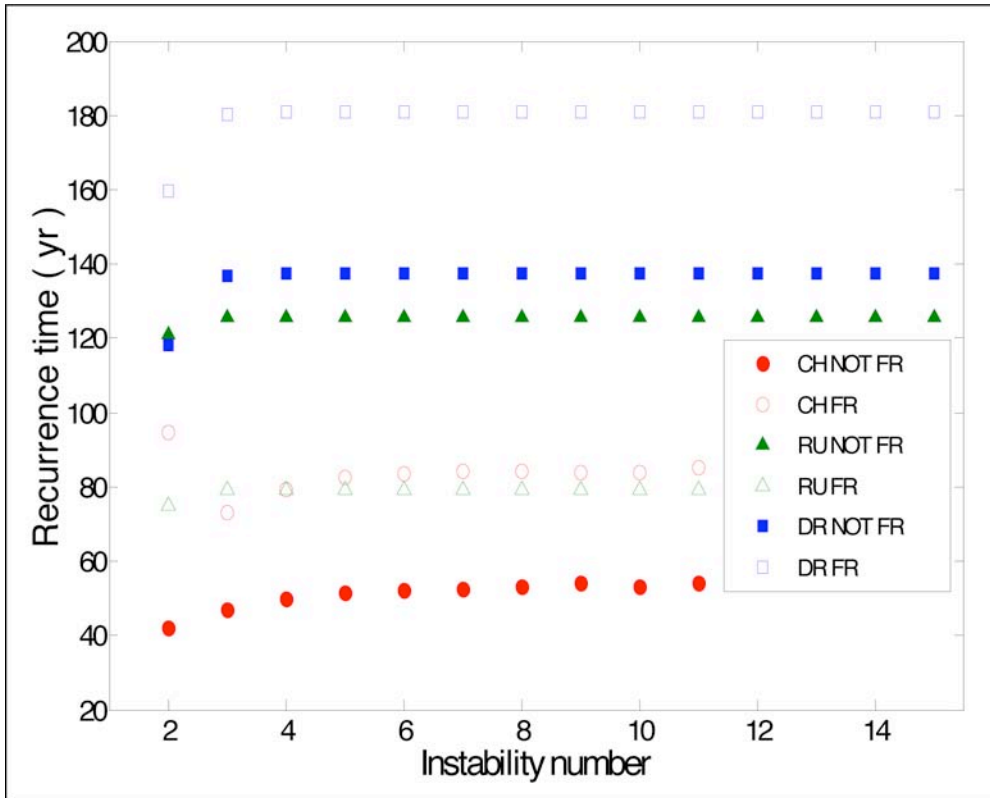


**Figure 4.** Recurrence time ( $T_{cycle}$ ) as resulting from the different governing models adopted in the present work. Open symbols refer to the frozen simulation while those closed refer to the not frozen simulation.

In addition, focusing on Figure 4, we can observe that the first instabilities (that are sensitive to the initial conditions of the system) become stable when the system reaches the limiting cycle.

In order to attribute a wider physical meaning to the previous numerical simulations and results, a further parametric investigation has been conducted. For instance, by considering the DR and RU *not frozen* simulations, a particular combination of the constitutive parameters  $a$ ,  $b$  and  $L$  has been sought for each constitutive law, keeping all the others parameters unchanged (initial velocity, loading rate, etc.), in order to achieve in both cases comparable  $T_{cycle}$  values.

Such numerical results are reported in Figure 5, where a similar seismic period, approximately 123

years, has been found for both the constitutive laws. Then it can be easily noted that the seismic cycle can be also strongly affected by the constitutive parameters chosen since it was possible to achieve compatible cycle times, nevertheless different constitutive laws have been considered.

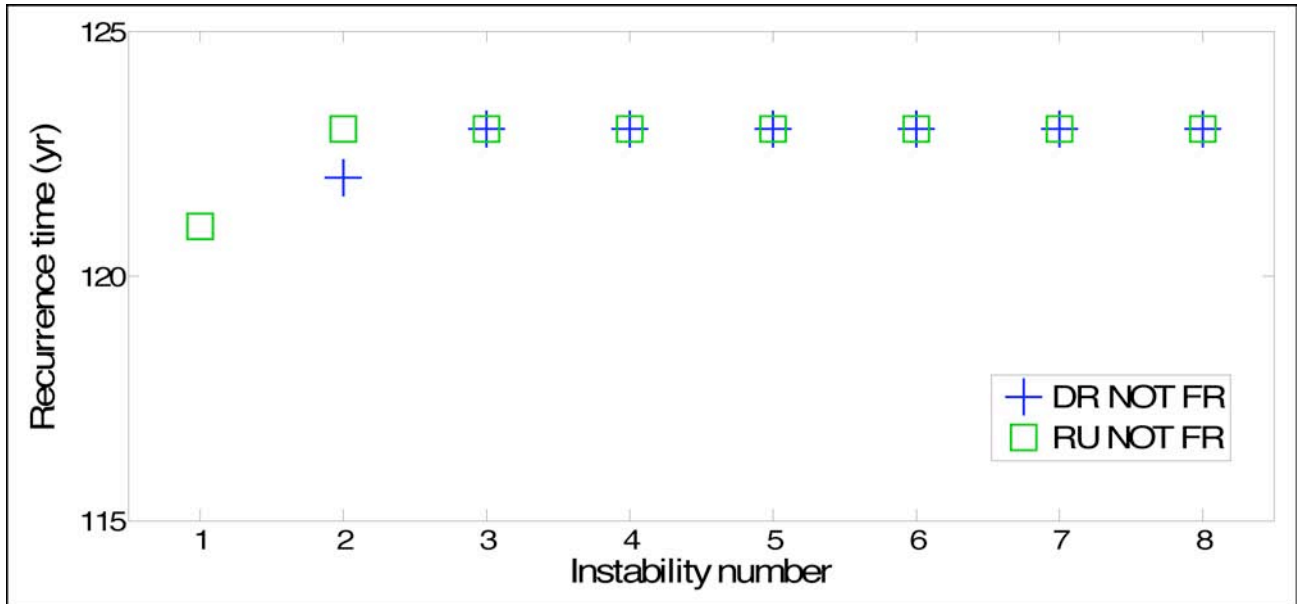


**Figure 5.** Comparable  $T_{cycle}$  (approximately 123 years) obtained by properly tuning the constitutive parameters of the DR and RU governing models in not frozen conditions. To obtain this result we adopted the following values:  $a = 0.007$ ,  $b = 0.016$ ,  $L = 1.5 \times 10^{-2}$  m for the DR law and  $a = 0.004$ ,  $b = 0.013$ ,  $L = 1.0 \times 10^{-2}$  m for the RU law, respectively.

In conclusion, through the observations conducted so far, it can be interestingly stated that the seismic cycle is affected by several aspects including the recovery time elapsed between two subsequent instabilities and the corresponding traction and slip velocity. Indeed, referring to the DR simulations of Figure 3, it was appreciated that in the case of relatively low shear stress a less evident velocity weakening effect occurs, although the corresponding slip velocity peaks were so high (Figure 2a). Consequently, this can result in a greater recovery time and then in a greater recurrence time of the earthquake ( $T_{cycle}$ ). Conversely, taking into account the CH simulations, higher traction peaks correspond to a stronger velocity weakening effect, which may produce a smaller recovery time and consequently also a lower seismic cycle.

#### 4. Summary

The sliding event on an interface generates frictional heating leading to a variation of the temperature field on the fault and on its surroundings. The incorporation of such a thermal effect within the dynamics of the sliding motion on active faults was the real improvement that Chester & Higgs carried out on the previous Dieterich-Ruina's and Ruina's constitutive formulations. Indeed, take into account the temperature change is extremely important in the dynamic modeling of seismic events, since there is a large number of thermally-activated physical and chemical phenomena which may occur during an earthquake rupture and may influence its dynamic propagation [Bizzarri, 2010a].

In this study we have mainly focused on the understanding of the effects that a particular rate- and state-constitutive law can exert on the seismic cycle span including its frozen and not frozen constrains.

In particular, we have compared three constitutive laws, the DR, the RU and the CH laws (sections 2.1, 2.2 and 2.3), in order to analyze their different ways of simulating the slip velocity and the shear stress time histories as well as the seismic cycle (recurrence time between subsequent failure events).

The analytical formulation of the above-mentioned friction laws has been obtained by considering laboratory data obtained at relatively low sliding speeds; recent laboratory data suggest that other formulations of the governing law should be used, in order to include additional dissipation phenomena occurring during the coseismic phase, such as the flash heating of micro-asperity contacts, the thermal pressurization of pore fluids, the hydrodynamic lubrication, the melting of rocks and gouge, etc. [see Bizzarri, 2010a for a review on this subject].

We perform numerical calculations with the spring-slider analog fault model, briefly summarized in section 1. This model of fault is somehow simplistic, in that it implicitly assumes that all the properties of the fault are homogeneous (and therefore the considered material point-like fault considered here is fully representative of all points of an extended seismogenic fault). Moreover, it neglects the effects due to the dynamic load exerted by the points of the fault that are already slipping and releasing stress (readers can refer to Bizzarri and Belardinelli, 2008 for a detailed discussion on this issue). Indeed, the mass-spring analog fault model is not able to simulate the radiation of seismic waves in the elastic medium, as more complete fault models do through the inclusion of the media which surround the fault [Bizzarri and Cocco, 2005 among many others].

Our numerical calculations demonstrate that the seismic cycle duration may depend on several factors:

- the specific analytical formulation rate- and state-dependent constitutive law considered to govern the seismogenic fault;
- the sliding velocity constrains, whether frozen or not frozen approximation is adopted;
- the adopted constitutive parameters ( $a$ ,  $b$  and  $L$ ).

Indeed, the behavior of a spring-slider system (and therefore the seismic cycle) also depends on the parameters of the model, such as the elastic constant of the spring, related to its critical value [e.g., Gu et al., 1984], vibration period and so on, as discussed in detail by Erickson et al. [2008].

In particular, our results clearly show that a spring-slider system governed by the CH constitutive law, compared to the DR and RU ones, needs a lower slip rate peak and a lower time interval to undergo to a seismic instability. Indeed, the earthquakes tend to occur earlier in the CH case probably because, such a constitutive model accounts for a further weakening effect due to the temperature evolution.

Finally, we have also seen that the not frozen simulations promote a time advance of a seismic event and also provides shorter seismic cycle times with respect to the frozen simulation for both the DR and the CH laws.

To finish, we want to highlight that the present results clearly demonstrate that the deterministic prediction of the earthquake occurrence — even in the simplest case of a single isolated fault with spatially homogeneous rheology — is markedly affected by the non obvious choice of the constitutive law which describes the time evolution of the frictional resistance. This has a clear impact within the seismic hazard assessment.



## References

- Belardinelli, M. E., A. Bizzarri, Cocco, M. (2003). Earthquake triggering by static and dynamic stress changes, *J. Geophys. Res.*, 108, No. B3, 2135, doi: 10.1029/2002JB001779.
- Bizzarri, A. (2010a). Toward the formulation of a realistic fault governing law in dynamic models of earthquake ruptures, in *Dynamic Modelling*, Edited by Alisson V. Brito, INTECH, Vienna, ISBN 978-953-7619-68-8, 167–188, <http://www.sciyo.com/articles/show/title/toward-the-formulation-of-a-realistic-fault-governing-law-in-dynamic-models-of-earthquake-ruptures>.
- Bizzarri, A. (2010b). Determination of the temperature field due to frictional heating on a sliding interface, *Rapporti Tecnici I.N.G.V.*, 158, 1–16.
- Bizzarri, A. (2010c). On the recurrence of earthquakes: Role of wear in brittle faulting, *Geophys. Res. Lett.*, 37, L20315, doi: 10.1029/2010GL045480.
- Bizzarri, A., Belardinelli, M. E. (2008). Modelling instantaneous dynamic triggering in a 3-D fault system: application to the 2000 June South Iceland seismic sequence, *Geophys. J. Int.*, 173, No. 3, 906–921, doi: 10.1111/j.1365-246X.2008.03765.x.
- Bizzarri, A., Cocco, M. (2005). 3D dynamic simulations of spontaneous rupture propagation governed by different constitutive laws with rake rotation allowed, *Ann. Geophys.*, 48, No. 2, 279–299.
- Carlson, J. M., Langer, J. S., Shaw, B. E. (1994). Dynamics of earthquake faults, *Rev. Modern Phys.*, 66, 657–670.
- Chester, F. M., Chester J. S. (1998). Ultracataclastic structure and friction processes of the Punchbowl fault, San Andreas system, California, *Tectonophys.*, 295, 199–221.
- Chester, F. M., Higgs, N. G. (1992). Multimechanism friction constitutive model for ultrafine gouge at hypocentral conditions, *J. Geophys. Res.*, 97, 1859–1870, doi: 10.1029/91JB02349.
- Dieterich, J. H. (1979). Modeling of rock friction, 1, Experimental results and constitutive equations, *J. Geophys. Res.*, 84, 2161–2168.
- Erickson, B., Birnir, B., Lavallée, D. (2008). A model for aperiodicity in earthquakes, *Nonlin. Processes Geophys.*, 15, 1–12.
- Gu, J. C., J. Rice, Ruina, A. L., Tse, S. T. (1984). Slip motion and stability of a single degree of freedom elastic system with rate and state dependent friction, *J. Mech. Phys. Solids*, 32, 167–196.
- Kato, N. (2001). Effect of frictional heating on pre-seismic sliding: a numerical simulation using a rate-, state- and temperature-dependent friction law, *Geophys. J. Int.*, 147, 183–188.
- Ruina, A. L. (1983). Slip instability and state variable friction laws, *J. Geophys. Res.*, 88, 10,359–10,370.
- Sibson, R. H. (2003), Thickness of the seismic slip zone, *Bull. Seism. Soc. Am.*, 93, No. 3, 1169–1178.
- Weeks, J. D. (1993). Constitutive laws for high-velocity frictional sliding and their influence on stress drop during unstable slip, *J. Geophys. Res.*, 98, 17,637–17, 648.



**Coordinamento editoriale e impaginazione**

Centro Editoriale Nazionale | INGV

**Progetto grafico e redazionale**

Daniela Riposati | Laboratorio Grafica e Immagini | INGV

© 2011 INGV Istituto Nazionale di Geofisica e Vulcanologia

Via di Vigna Murata, 605

00143 Roma

Tel. +39 06518601 Fax +39 065041181

**<http://www.ingv.it>**



**Istituto Nazionale di Geofisica e Vulcanologia**